Journal of Computational Science & Engineering 12 (2014) 445-451

Journal of Computational Science & Engineering

Available at http://www.asocse.org ISSN 1710-4068

Impacts of PHEV Driving Types on Electro-hydraulic Braking

Jinlong Liu[1*], Xiaoyu Zhang[2], Rui Huang[3]

[1]*School of Automotive Engineering, Harbin Institute of Technology, 264209, Weihai Shandong China*
[2]*School of Astronautics, Harbin Institute of Technology, 150001, Harbin Heilongjiang China*
[3]*China Automotive Engineering Research Institute Co., Ltd., 401122, Chongqing China*

Article Information

Article history:
Received 5 May 2014
Revised 23 May 2014
Accepted 31 May 2014
Available online 3 June 2014

Keywords:
Electro-hydraulic braking
Ideal braking force distribution
Regenerative braking
Recovery rate
Driving types

Abstract

As automotive by-wire control technology matures, the electro-hydraulic braking technique in Parallel Hybrid Electric Vehicles (PHEV) can achieve the goal of ideal braking force distribution in front and rear wheels. In order to discuss the impacts of PHEV driving types on recovery rate of electro-hydraulic regenerative braking, theoretical analyses of PHEV were done on the flat and level road. Then the braking models were established on the platform of Matlab/Simulink and at the same time they were simulated with certain parameters. The results indicate that the four wheel drive (4WD) pattern has higher efficiency than the two wheel drive (2WD) in regenerative braking and that whether the front wheel drive (FWD) pattern is better than rear wheel drive (RWD) pattern in regenerative braking depends on the main vehicle parameters and pavement friction coefficient.

1. Introduction

Currently, traditional internal combustion engine vehicles have contributed to lots of environmental problems, ranging from the air deterioration to the scarce of fuel resources [1]. Additionally, difficulties in cells restrict the development of electric vehicles [2]. Thus the PHEV is becoming the hottest topic in automotive industry [3]. The electro-hydraulic technology made it possible for PHEV to distribute the braking forces in an ideal

* Corresponding author: ljl199022@sina.com

2014 © The American Computational Science Society. All rights reserved.

pattern [4]. In this pattern, the braking forces are provided by the motor when the expected severity of braking is lower than 0.1 and the braking forces are composed of regenerative braking forces and mechanical braking forces when the expected severity of braking is higher than 0.1. In order to reduce the complexity without influencing the conclusions, the braking forces in the discussion are always the sum of regenerative braking forces and mechanical braking forces.

2. Ideal braking force distribution theory

Before discussing the ideal braking force distribution, force conditions of PHEV are analyzed on the flat and level road. Figure 1 shows the force model of PHEV. In this model, the rolling moment of couple, air resistance and inertia moment of couple are neglected [5]. In addition, the process of rolling and slipping is also ignored. Thus the pavement adhesion coefficient can be regarded as a constant value.

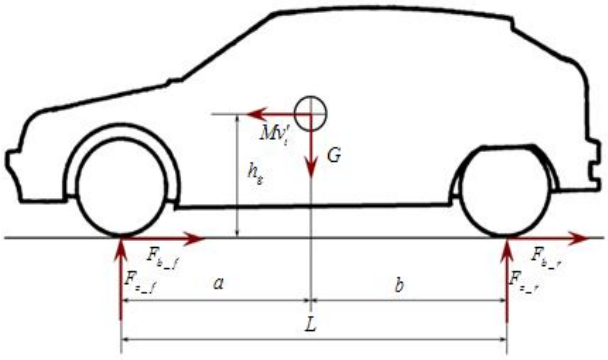

Fig.1 PHEV force model

Based on the equilibrium analysis, the equation can be concluded.

$$F_{b_f} + F_{b_r} = F_{b_sum} = Gv_t' / g \quad (1)$$

As is shown in Eq.1, F_{b_f} is the ground friction on front wheels; F_{b_r} is the ground friction on rear wheels; F_{b_sum} is the total ground friction; G is the gravity of PHEV; g is the acceleration of gravity; v_t is the instantaneous vehicle velocity.

The severity of braking is one of the evaluating indexes in braking efficiency.

$$z = v_t' / g \quad (2)$$

As is shown in Eq.2, z is the severity of braking.

Eq.3 is concluded through the moment-equilibrium on the ground point of rear wheel.

$$F_{z_f} = \frac{Gb + mv_t'h_g}{L} = \frac{G}{L}\left(b + zh_g\right) \quad (3)$$

As is shown in Eq.3, F_{z_f} is the normal force of front wheels provided by the ground; L is the wheel base of vehicle; b is the distance between center of mass and front axle; h_g is the height of center of mass.

Eq.4 is concluded through the moment-equilibrium on the ground point of front wheel.

$$F_{z_r} = \frac{Ga - mv_t'h_g}{L} = \frac{G}{L}\left(a - zh_g\right) \quad (4)$$

As is shown in Eq.4, F_{z_r} is the normal force of rear wheels provided by the ground; a is the distance between center of mass and rear axle.

When the front wheels and the rear wheels lock at the same time, the relation between front braking forces and rear braking forces is the ideal distribution.

$$F_{b_f} + F_{b_r} = \varphi G \quad (5)$$

$$\frac{F_{b_f}}{F_{b_r}} = \frac{b + \varphi h_g}{a - \varphi h_g} \quad (6)$$

As is shown in Eq.5 and Eq.6, φ is the pavement adhesion coefficient.

Eq.7 can be concluded by eliminating the variable φ.

$$F_{b_r} = \frac{1}{2}\left[\frac{G}{h_g}\sqrt{b^2 + \frac{4h_gL}{G}F_{b_f}} - \left(\frac{Gb}{h_g} + 2F_{b_f}\right)\right] \quad (7)$$

2.1. FWD pattern

For the FWD pattern of PHEV, the regenerative braking forces provided by the motor are applied on the front wheels. During the operation, the motor cannot provide the maximum allowed instantaneous front braking forces all the time. The

2014 © The American Computational Science Society. All rights reserved.

participant regenerative braking forces are shown in Eq.8.

$$F_{b_f_re}=\begin{cases}F_{re_a} & F_{re_a}\le F_{b_f}\\ F_{b_f} & F_{re_a}>F_{b_f}\end{cases} \quad (8)$$

As is shown in Eq.8, $F_{b_f_re}$ is the regenerative braking force in FWD pattern; F_{re_a} is the maximum instantaneous regenerative braking force that can be provided by the motor.

The Eq.9 and Eq.10 show the instantaneous mechanical braking forces during the braking process.

$$F_{b_f_me}=F_{b_f}-F_{b_f_re} \quad (9)$$

$$F_{b_r_me}=F_{b_r} \quad (10)$$

As is shown in Eq.9 and Eq.10, $F_{b_f_me}$ is the instantaneous mechanical braking force of front wheels; $F_{b_r_me}$ is the instantaneous mechanical braking force of rear wheels.

2.2. RWD pattern

For the RWD pattern of PHEV, the regenerative braking forces provided by the motor are applied on the rear wheels. During the operation, the motor cannot provide the maximum allowed instantaneous rear braking forces all the time. The participant regenerative braking forces are shown in Eq.11.

$$F_{b_r_re}=\begin{cases}F_{re_a} & F_{re_a}\le F_{b_r}\\ F_{b_r} & F_{re_a}>F_{b_r}\end{cases} \quad (11)$$

As is shown in Eq.11, $F_{b_r_re}$ is the regenerative braking force in RWD pattern.

The Eq.12 and Eq.13 show the instantaneous mechanical braking forces during the braking process.

$$F_{b_f_me}=F_{b_f} \quad (12)$$

$$F_{b_r_me}=F_{b_r}-F_{b_r_re} \quad (13)$$

2.3. 4WD pattern

For the 4WD pattern of PHEV, the regenerative braking forces provided by the motor are applied both on the front and the rear wheels. The 4WD pattern PHEV is able to adjust the distribution ratio of front regenerative braking forces to rear regenerative braking forces according to different conditions. The participant regenerative braking forces are shown in Eq.14.

$$F_{b_r_re}+F_{b_r_re}=\begin{cases}F_{re_a}, & F_{re_a}\le F_{b_f}+F_{b_r}\\ F_{b_f}+F_{b_r}, & F_{re_a}>F_{b_f}+F_{b_r}\end{cases} \quad (14)$$

The Eq.15 and Eq.16 show the instantaneous mechanical braking forces during the braking process.

$$F_{b_f_me}=F_{b_f}-F_{b_f_re} \quad (15)$$

$$F_{b_r_me}=F_{b_r}-F_{b_r_re} \quad (16)$$

2.4. Effects of driving types

For the PHEV used electro-hydraulic braking technique, the instantaneous braking force distribution coefficient can be concluded when the driver is stepping on the brake.

$$\beta_t(t)=\frac{\hat{\varphi}(t)h_g+b}{L} \quad (17)$$

As is shown in Eq.17, $\beta_t(t)$ is the instantaneous braking force distribution coefficient; $\hat{\varphi}(t)$ is the instantaneous equivalent pavement friction coefficient corresponding to the driver's brake operation.

During this process, the instantaneous braking forces of front and rear wheels are shown in Eq.18 and Eq.19.

$$F_{b_f_\hat{\varphi}}=\beta_t(t)\hat{\varphi}(t)G=\frac{b+\hat{\varphi}(t)h_g}{L}\hat{\varphi}(t)G \quad (18)$$

$$F_{b_r_\hat{\varphi}}=\left(1-\beta_t(t)\right)\hat{\varphi}(t)G=\frac{a-\hat{\varphi}(t)h_g}{L}\hat{\varphi}(t)G \quad (19)$$

When the car is running on the ground with pavement friction coefficient of φ_0 and both the front and the rear wheels are locked, the braking force distribution coefficient is shown in Eq.20.

$$\beta_0=\frac{\varphi_0 h_g+b}{L} \quad (20)$$

At this time, the braking forces of front and rear wheels are shown in Eq.21 and Eq.22.

$$F_{b_f_\varphi_0}=\beta_0\varphi_0 G=\frac{b+\varphi_0 h_g}{L}\varphi_0 G \quad (21)$$

$$F_{b_r_\varphi_0}=\left(1-\beta_0\right)\varphi_0 G=\frac{a-\varphi_0 h_g}{L}\varphi_0 G \quad (22)$$

During the whole braking process, the front

2014 © The American Computational Science Society. All rights reserved.

braking energies is shown in Eq.23.

$$W_f = \int_0^{\varphi_0} F_{b_f_\hat{\varphi}} S(\hat{\varphi}) d\hat{\varphi} + F_{b_f_\varphi_0} S_0 = \int_0^{\varphi_0} \frac{b + \hat{\varphi}(t) h_g}{L} \hat{\varphi}(t) GS(\hat{\varphi}) d\hat{\varphi} + \frac{b + \varphi_0 h_g}{L} \varphi_0 GS_0 \quad (23)$$

As is shown in Eq.23, $S(\hat{\varphi})$ is the instantaneous braking distance when the braking forces are rising; S_0 is the braking distance when all the wheels are locked.

During the whole braking process, the front braking energies is shown in Eq.24.

$$W_r = \int_0^{\varphi_0} F_{b_r_\hat{\varphi}} S(\hat{\varphi}) d\hat{\varphi} + F_{b_r_\varphi_0} S_0 = \int_0^{\varphi_0} \frac{a - \hat{\varphi}(t) h_g}{L} \hat{\varphi}(t) GS(\hat{\varphi}) d\hat{\varphi} + \frac{a - \varphi_0 h_g}{L} \varphi_0 GS_0 \quad (24)$$

During the whole braking process, the total braking energies is shown in Eq.25.

$$W_{sum} = W_f + W_r \quad (25)$$

As is shown in Eq.25, W_{sum} is higher than W_f and W_{sum} is also higher than W_r. Thus the PHEV with 4WD pattern has more opportunities in recovering braking energies than the PHEV with 2WD pattern. So the 4WD pattern can recover more braking energies than the FWD pattern and the RWD pattern.

Eq.26 shows the difference between front braking energies and rear braking energies.

$$W_f - W_r = \int_0^{\varphi_0} \frac{b - a + 2\hat{\varphi}(t) h_g}{L} \hat{\varphi}(t) GS(\hat{\varphi}) d\hat{\varphi} + \frac{b - a + 2\varphi_0 h_g}{L} \varphi_0 GS_0 \quad (26)$$

As is shown in Eq.26, $W_f - W_r > 0$ when $b - a \geq 0$. So at this time the PHEV with FWD pattern has more opportunities in recovering braking energies than the PHEV with RWD pattern.

When $b - a \geq 0$, Eq.27 exists during the whole braking process.

$$F_{b_f} > F_{b_r} \quad (27)$$

Eq.28 can be concluded according to the Eq.27.

$$F_{b_f_re} > F_{b_r_re} \quad (28)$$

Eq.29 shows the difference between front recovery energies in FWD pattern and rear recovery energies in RWD pattern.

$$W_{f_re} - W_{r_re} = \int F_{b_f_re} dS - \int F_{b_r_re} dS > 0 \quad (29)$$

According to Eq.29, it can be also concluded that the FWD pattern can recover more braking energies than the RWD pattern when $b - a \geq 0$.

When $b - a + 2\varphi_0 h_g \leq 0$, it can be concluded that $W_f - W_r < 0$. At this time the PHEV with RWD pattern has more opportunities in recovering braking energies than the PHEV with FWD pattern. It can be also concluded that the pavement friction coefficient affects this advantage.

When $b - a < 0$ and $b - a + 2\varphi_0 h_g > 0$ or when $-2\varphi_0 h_g < b - a < 0$, whether FWD pattern can recover more braking energies than RWD pattern is uncertain. The relations between them associate with pavement friction coefficient and operations of the driver.

3. Results and discussion

3.1 Braking models of PHEV

The braking models of PHEV are built on the platform of Matlab/Simulink.

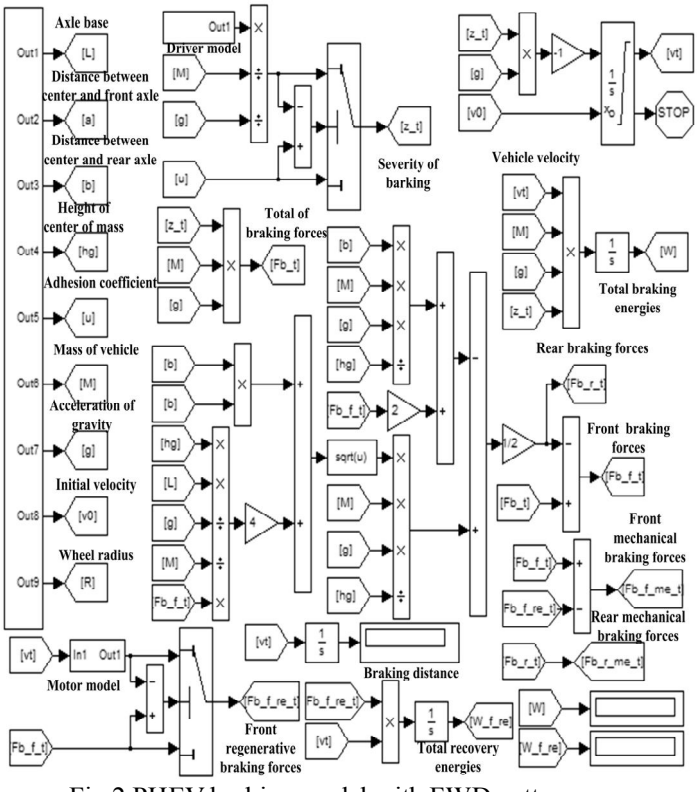

Fig.2 PHEV braking model with FWD pattern

Figure 2 shows the PHEV braking model with

2014 © The American Computational Science Society. All rights reserved.

FWD pattern. The instantaneous front and rear braking forces are calculated according to the ideal distribution theory. The expected braking requirements are judged by the brake pedal stroke and the pressing speed in the module of driver. The instantaneous braking severity of PHEV can be decided by the comparison between the expected braking requirements and the pavement adhesion coefficient. The PHEV instantaneous velocity is calculated according to the instantaneous braking severity. The total braking energies are calculated with the help of instantaneous velocity and the braking severity. The motor module uses the DC motor with separated excitation. The rotate speed of motor output can be calculated according to the gear ratio and PHEV instantaneous velocity. Thus the regenerative braking torques can be calculated. Then the available braking forces provided by the motor can be concluded by the gear ratio and wheel radius. The real front braking forces provided by the motor can be calculated through the comparison between the demand of front braking forces and the motor available braking forces. The total available recovered energies can be calculated according to the real front motor braking forces and the PHEV velocity. The front mechanical braking forces can be calculated through the subtraction between the wanted front braking forces and the real front motor braking forces. The rear mechanical braking forces equals the wanted rear braking forces. The braking distance is calculated through the integration of the PHEV instantaneous velocity. The whole model requiring parameters are input through parameter definition module.

Figure 3 shows the PHEV braking model with RWD pattern. The real rear braking forces provided by the motor can be calculated through the comparison between the demand of rear braking forces and the motor available braking forces. The total available recovered energies can be calculated according to the real rear motor braking forces and the PHEV velocity. The rear mechanical braking forces can be calculated through the subtraction between the wanted rear braking forces and the real rear motor braking forces. The front mechanical braking forces equals the wanted front braking forces. The rest modules in the RWD model use the same counterparts in the FWD model.

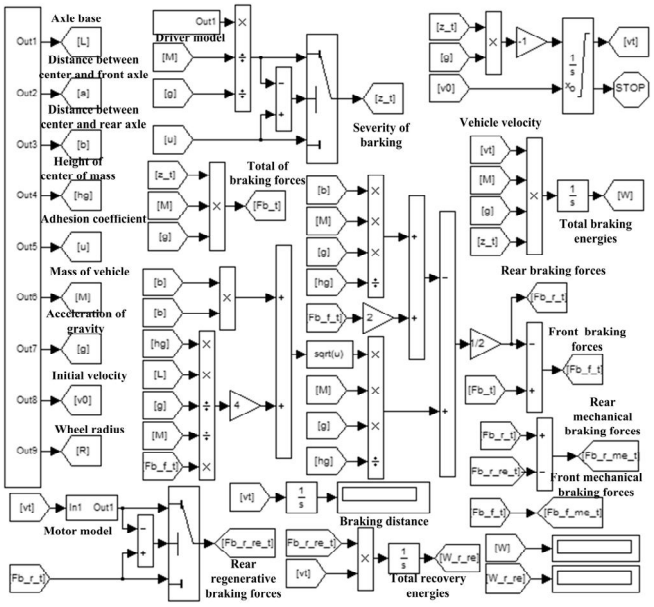

Fig.3 PHEV braking model with RWD pattern

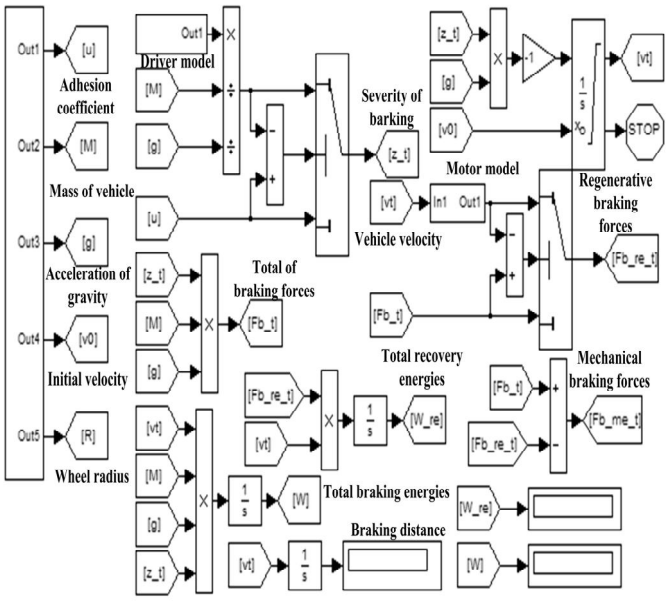

Fig.4 PHEV braking model with 4WD pattern

Figure 4 shows the PHEV braking model with 4WD pattern. The real braking forces provided by the motor can be calculated through the comparison between the demand of total braking forces and the motor available braking forces. The total available recovered energies can be calculated according to the real motor braking forces and the PHEV velocity. The total mechanical braking forces can

2014 © The American Computational Science Society. All rights reserved.

be calculated through the subtraction between the wanted total braking forces and the real motor braking forces. The rest modules in the 4WD model use the same counterparts in the FWD model or the RWD model.

3.2. Analyses of simulation results

These three models embed with certain PHEV parameters are simulated. Table 1 shows the PHEV and the pavement parameters. Table 2 shows the simulation results.

Table 1 The input parameters

Parameters	Value
Wheel base of PHEV [m]	2.6
Distance between front axle and the mass center [m]	1.04
Distance between rear axle and the mass center [m]	1.56
Height of center of mass [m]	0.5
Mass of PHEV [kg]	1600
Acceleration of gravity [N/kg]	9.8
Wheel radius [m]	0.25
Power of motor [kW]	30
Pavement friction coefficient	0.65

Table 2 Recovery rate results

Initial velocity [km/h]	FWD pattern	RWD pattern	4WD pattern
70	10.82%	10.59%	10.97%
60	10.69%	10.67%	10.71%
50	12.86%	12.15%	13.28%
40	10.81%	10.60%	10.96%
30	16.01%	15.05%	16.02%

From the table 2, it can be concluded that the FWD pattern recovers more braking energies than the RWD pattern. And at this time, the distance between front axle and mass center is shorter than the distance between rear axle and mass center. In addition, the 4WD pattern recovers more braking energies than the FWD (or RWD) pattern.

These three models embed with another PHEV parameters are also simulated. Table 3 shows the PHEV and the pavement parameters. Table 4 shows the simulation results.

Table 3 The input parameters

Parameters	Value
Wheel base of PHEV [m]	5.6
Distance between front axle and the mass center [m]	3.733
Distance between rear axle and the mass center [m]	1.867
Height of center of mass [m]	1
Mass of PHEV [kg]	5800
Acceleration of gravity [N/kg]	9.8
Wheel radius [m]	0.52
Power of motor [kW]	30
Pavement friction coefficient	0.65

Table 4 Recovery rate results

Initial velocity [km/h]	FWD pattern	RWD pattern	4WD pattern
70	3.92%	4.00%	4.03%
60	4.28%	4.29%	4.30%
50	5.34%	5.58%	5.66%
40	4.38%	4.46%	4.49%
30	8.54%	8.73%	8.73%

From the table 4, it can be concluded that the RWD pattern recovers more braking energies than the FWD pattern. And at this time, the sum of the distance between rear axle and mass center and the twofold product of pavement friction coefficient and height of center of mass is shorter than the distance between front axle and mass center. In addition, the 4WD pattern recovers more braking energies than the FWD (or RWD) pattern.

4. Conclusion

The relations between the driving types and the recovery rate of regenerative brake of electro-hydraulic braking in PHEV are analyzed both in theoretical derivations and computer simulations. The results show that the 4WD pattern is able to recover more braking energies than the FWD (or RWD) pattern. Besides, the FWD pattern recovers more braking energies than the RWD pattern when the distance between front axle and

2014 © The American Computational Science Society. All rights reserved.

mass center is shorter than the distance between rear axle and mass center. In addition, the RWD pattern recovers more braking energies than the FWD pattern when the sum of the distance between rear axle and mass center and the twofold product of pavement friction coefficient and height of center of mass is shorter than the distance between front axle and mass center. However, there are also some shortcomings in the discussions. For example, the whole analyses were only done on the flat and level road. In the future, the whole analyses would take the upgrade and downgrade situations into consideration.

References

[1] J.L. Liu, J.M. Zhang, M.Z. Xue, Journal of applied science and engineering innovation, 4 (2014) 260-267.
[2] J.L. Liu, J.M. Zhang, Z.W. Gao, Journal of applied science and engineering innovation, 4 (2014) 251-259.
[3] J.L. Liu, J.M. Zhang, M.Z. Xue, Applied Mechanics and Materials, 536 (2014) 1065-1068.
[4] J.M. Zhang, J.L. Liu, M.Z. Xue, Advanced Materials Research, 926 (2014) 743-746.
[5] J.L. Liu, Z.W. Gao, J.M. Zhang, Advanced Materials Research, 926 (2014) 896-900.

2014 © The American Computational Science Society. All rights reserved.